Tricriticality in the Orientational Phase Diagram of Stepped Si(113) Surfaces

S. Song and S. G. J. Mochrie
Department of Physics, Massachusetts Institute of Technology, Cambridge, Massachusetts 02139-4307
(Received 17 May 1994)

An x-ray scattering study is presented of the orientational phase diagram of Si surfaces misoriented by up to 6° from the cubic [113] direction towards [001] and for temperatures between 300 and 1500 K. At the highest temperatures, the surface is uniformly stepped. Below $T_t = 1223$ K, there is a two-phase region in which (113) facets appear in coexistence with the stepped phase. We identify T_t as a tricritical point. For temperatures between a triple point at $T_3 = 1134$ K and 300 K, coexistence between the (113) facet and the (114) facet is found.

PACS numbers: 68.35.Rh, 61.10.Lx, 64.70.Kb

Our present understanding of surface morphology depends crucially on understanding the fluctuations and interactions of steps [1–7]. In the present paper, we report the observation of a new critical behavior among steps on a crystal surface, yielding new insight into these topics. Specifically, we describe an x-ray scattering study of the orientational phase diagram of stepped Si surfaces miscut away from the [113] direction towards [001]. Remarkably, we find strongly temperature-dependent diffuse scattering, reminiscent of critical scattering. The diffuse scattering is a result of step fluctuations, and foreshadows a faceting transformation, at which the surface transforms from a homogeneous phase of uniform orientation (or step density) into coexisting phases with different orientations. The faceting transformation found here is quite distinct from those previously observed, where faceting is induced by a first-order transformation between different surface phases [5–7], such as reconstructed and unreconstructed phases. In contrast, our results suggest that faceting of stepped Si(113) is a consequence of a direct attractive interaction between steps.

In fact, the diffuse scattering may be associated with a *tricritical point* in the orientational phase diagram, at which the transformation between the stepped phase and the (113) facet changes from continuous to first order, as the effective interaction between steps changes from repulsive to attractive [1–3]. Aspects of the observed behavior may be understood qualitatively on the basis of a simple mean-field theory. However, the measured values of the tricritical exponents remain unexplained.

The proposed orientational phase diagram is shown in Fig. 1. Solid lines indicate phase boundaries, while solid circles and squares represent microscopic surface orientations measured for samples with macroscopic misorientations of 2.1° and 3.7°, respectively. Previous work has revealed that the (113) facet, located at zero misorientation angle, is a stable phase for all temperatures shown [8]. At nonzero misorientation angles and for temperatures above 1223 K, there occurs a one-phase region of the phase diagram (shown hatched in Fig. 1), in which the surface is uniformly stepped. We infer that there is a continuous transformation versus orientation between the stepped phase and the (113) facet above 1223 K [1–3]. It is striking that in this region the intensity of the near-specular, diffuse scattering increases as the temperature is decreased towards 1223 K. Between 1223 and 1134 K, there is a two-phase region (unhatched) in which (113) facets appear in coexistence with the stepped phase, so that the transformation versus orientation between the stepped phase and the (113) facet is first order. Thus, $T_t = 1223$ K is a tricritical point (open square in Fig. 1). The range of angles forbidden to the stepped phase in-

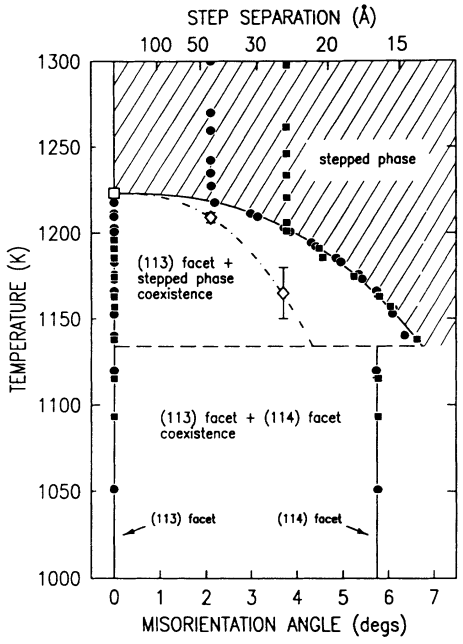

FIG. 1. Orientational phase diagram of stepped Si(113) surfaces with misorientation angles towards [001]. The one-phase region is hatched; two-phase regions are unhatched. Solid lines are phase boundaries. Solid circles and solid squares show the misorientation angles measured for the 2.1° miscut sample, and the 3.7° miscut sample, respectively. The open square is the tricritical point. The dashed line corresponds to the triple point. The diamonds and the dot-dashed line represent the spinodal line described in the text.

creases continuously with decreasing temperature, reaching an angle of 6.4° by 1134 K. The (113) facet itself does not undergo a transformation at T_t [8], in contrast to the behavior found at previously described faceting transformations [5–7]. [The (113) facet exhibits a continuous transformation to a (3×1) phase below $T_c = 960$ K [8].] Below a triple point temperature of $T_3 = 1134 \pm 6$ K (dashed line in Fig. 1), coexistence between the (113) facet and the (114) facet, which lies 5.7° from the [113] direction, replaces coexistence between the (113) facet and the stepped phase.

We studied n-type silicon wafers with surface normals miscut by 2.1° and 3.7° away from [113] towards [001]. Direct current through the sample provided resistive heating, and also a measure of the temperature. The absolute temperature was given by a calibrated optical pyrometer. The precision of the relative temperature measurement and control was 1 K, while we estimate the absolute accuracy to be 40 K. In the following, we quote relative errors in temperature. Samples were cleaned in UHV by repeated annealing at 1535 K for 1 min, with the pressure remaining below 1×10^{-9} Torr [9]. During the measurements, the pressure remained less than 3×10^{-10} Torr. The diffraction pattern and phase behavior were routinely reproducible, and Auger electron spectroscopy indicated a clean surface.

We use a rectangular coordinate system to index reciprocal space. Referred to the cubic reciprocal lattice of Si, the reciprocal lattice vectors defining the H, K, and L directions are $(1,\bar{1},0)/2$ with magnitude $a^* = 1.64$ Å^{-1}, $(3,3,\bar{2})/2$ with magntitude $b^* = 0.49$ Å^{-1}, and $(1,1,3)/11$ with magnitude $c^* = 0.35$ Å^{-1}, respectively. The measurements were carried out at beam lines X20A and X25 at the National Synchrotron Light Source (NSLS) using x rays with an energy of 8 keV.

Scattering from the 2.1° miscut sample at 1252 K is illustrated in Fig. 2(a). These scans were taken at different values of L near the condition for specular x-ray reflection. In each profile, there appears a single peak, the location of which shifts linearly in K with increasing L. Thus, the scattering comprises a rod of scattering, tilted away from the L direction by an angle equal to $\theta = \tan^{-1}(-Kb^*/Lc^*) = 2.1°$. The tilt angle of the rod yields the misorientation of the surface normal with respect to the [113] direction. Evidently, at this temperature the surface lies in a one-phase region of the orientational phase diagram.

The full width at half maximum (FWHM) of each of the scans in Fig. 2(a) is $0.0037b^* = 0.0018$ Å^{-1}, corresponding to the instrumental resolution for the data shown. In addition to a resolution-limited peak located at the specular condition, diffuse scattering may be seen decreasing slowly in intensity away from the peak. The solid lines in Fig. 2(a) correspond to the theoretical line shape expected for a stepped phase taking into account the experimental resolution [10]. Specifically, the line

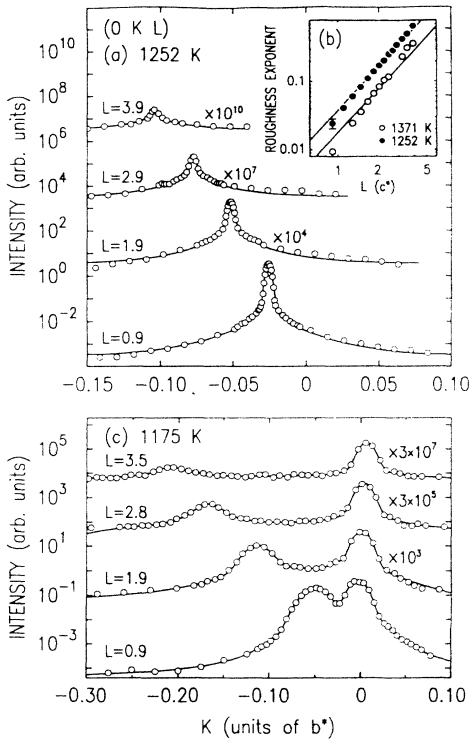

FIG. 2. Near-specular scans along the K direction at several different values of L for the 2.1° miscut sample. (a) Scans obtained at 1252 K. Solid lines correspond to the model line shape described in the text. (b) Roughness exponent vs L for 1252 K (solid circles) and 1371 K (open circles). Solid lines are the best fit to a quadratic dependence on L. (c) Scans obtained at 1175 K. Solid lines are guides to the eye.

shape versus K is modeled as

$$\frac{I_K}{I} = \frac{\Delta Q_y}{2\pi} \int dy\, e^{i\kappa b^* y} e^{-\Delta Q_y^2 y^2/4\pi} e^{-Q_z^2 g(y,0)/2}, \quad (1)$$

with the height difference correlation function given by $g(y,0) = (k_B T/\pi\tilde{\gamma})[\ln(y/\xi) + K_0(y/\xi) - 0.115\,93]$, where $\tilde{\gamma}$ is the surface stiffness [10]. K_0 is a modified Bessel function, $Q_y = Kb^*$, $Q_z = Lc^*$, and $\kappa = (Q_y + Q_z \tan\theta)/b^*$ is the displacement along K from the specular condition in units of b^*. This description leads to a line shape that may be characterized by a quantity $k_B T Q_z^2/2\pi\tilde{\gamma}$, which we call the roughness exponent. A large value of the roughness exponent corresponds to intense near-specular, diffuse scattering. For a stepped surface, the correlation length (ξ) is expected to be proportional to the step separation [11], which is 44 Å for the 2.1° miscut surface. Accordingly, we describe the results of fits for which ξ was fixed at 44 Å. The parameters varied in the fits were the integrated intensity (I), the roughness exponent, and the intensity of background scattering from the bulk. Equation (1) provides an excellent description of the observed scattering throughout the range of K and L studied both at 1252 K [Fig. 2(a)] and at 1371 K (data not shown).

Moreover, our results for the roughness exponent do not depend sensitively on ξ. Figure 2(b) shows the roughness exponent versus L at 1252 and 1371 K for the 2.1° miscut sample on a log-log scale. The variation is well described by a quadratic form [solid lines in Fig. 2(b)], confirming that Eq. (1) is an appropriate description of the observed scattering at these temperatures.

Comparable scans obtained at 1175 K are shown in Fig. 2(c). However, in each of these profiles, there are two peaks. One of the peaks shifts linearly to smaller K as L increases. By contrast, the other peak occurs at a fixed value of $K = 0$, independent of L. Clearly, at this temperature the scattering comprises two rods. We deduce that the surface morphology consists of (113) facets in coexistence with stepped regions, oriented away from the [113] direction by 5.3°. The peaks seen in Fig. 2(c) are considerably broader than those of Fig. 2(a). Specifically, the FWHM of the peak corresponding to the (113) facet is $0.020b^* = 0.010$ Å^{-1}, and that of the stepped phase is $0.030b^* = 0.015$ Å^{-1}. The peak widths are independent of L in both cases. We estimate that the sizes of the (113) facets and of the stepped regions along the K direction are on average 600 Å and 400 Å, respectively.

How the surface morphology changes with temperature is clarified in Fig. 3, which shows scans along the K direction at $L = 2.0$ for several different temperatures between 1505 and 881 K. Above 1220 K, the profile consists of a single peak, indicating a surface orientation conforming to the macroscopic miscut of 2.1°. Below 1220 K, however, a peak appears at $K = 0$ and grows in intensity, corresponding to the appearance of (113) facets on the sample surface. In addition, the position of the stepped-phase peak shifts continuously to smaller values of K, indicating a continuous increase in the misorientation angle for temperatures decreasing below 1220 K. In the context of the orientational phase diagram, the misorientation angle observed below 1220 K constitutes the boundary between one- and two-phase regions. In fact, the misorientation angle (θ) follows a power law versus reduced temperature [$t = (T_t - T)/T_t$]: $\theta = \theta_0 t^\beta$, with $\beta = 0.42 \pm 0.10$, $\theta_0 = 21 \pm 6°$, and $T_t = 1223 \pm 2$ K. This is shown as a solid line in Fig. 1. We interpret β as a tricritical exponent.

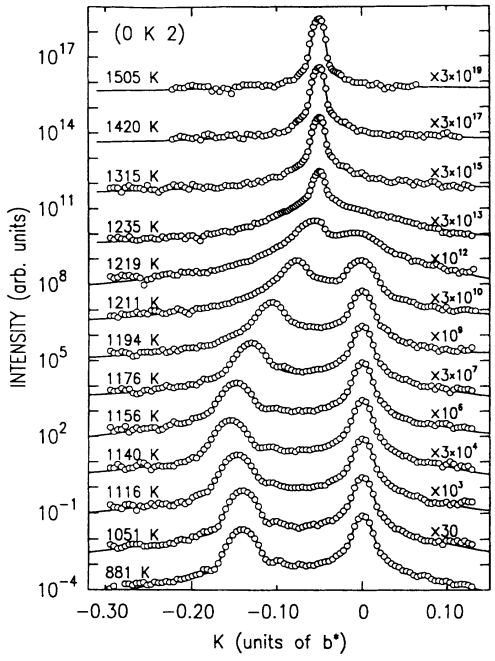

FIG. 3. Near-specular scans along the K direction at $L = 2$ for temperatures between 1505 and 881 K. Solid lines for temperatures above T_t correspond to the model described in the text. Solid lines for temperatures below T_t are guides to the eye.

It may be seen from Fig. 3 that the intensity of the diffuse scattering increases as the temperature is decreased towards T_t. To quantify the diffuse scattering, the profiles obtained in the one-phase region were fitted by Eq. (1). The resolution was fixed to be $0.0089b^*$ FWHM, appropriate for the data of Fig. 3, and ξ was fixed to be 44 Å. Very close to T_t, broad scattering appears along the [113] direction ($K = 0$), giving rise to a slight apparent asymmetry about the peak position. As a result, to describe the data, it is necessary to incorporate an additional, broad peak in the model, located at $K = 0$. The intensity of this peak does not strongly affect our results for the roughness exponent, but nevertheless contributes to the uncertainty. The solid lines in Fig. 3 illustrate the best fit profiles. For the 3.7° miscut sample, fits were performed with ξ fixed at 26 Å (data not shown).

The dramatic increase in the intensity of the diffuse scattering as the temperature is decreased towards T_t is highlighted in Fig. 4(a), which reproduces on a log-log scale versus κ, the intensity at $L = 2.0$, obtained in the one-phase region at several different temperatures. Also illustrated are the corresponding model profiles, which evidently provide an excellent description of the data. The data shown correspond to values of K more negative than at the peak. Figure 4(b) summarizes our results for the surface stiffness versus reduced temperature $\{s(\theta) = [T - T_s(\theta)]/T_s(\theta)\}$ on a log-log scale, deduced from fits of Eq. (1) to data obtained in the one-phase region. Open triangles and open circles correspond to data obtained for the 2.1° miscut sample, and illustrated in Figs. 2(a) and 4(a), respectively. Solid circles correspond to data obtained for the 3.7° miscut sample. The linear behavior evident in Fig. 4(b) for reduced temperatures less than about 0.1 suggests that the surface stiffness decreases as a power of the reduced temperature near the transformation, i.e., $\tilde{\gamma} = \tilde{\gamma}_0 s^\lambda$. The best fit for reduced temperatures less than 0.1 yields the solid line shown, for which $\lambda = 0.76 \pm 0.2$, $\tilde{\gamma}_0 = 56 \pm 20$, and $T_s(2.1°) = 1206 \pm 3$ K, and $T_s(3.7°) = 1165 \pm 15$ K; λ is a second tricritical exponent. We show $T_s(2.1°)$ and $T_s(3.7°)$ in Fig. 1 as open diamonds. The accompanying

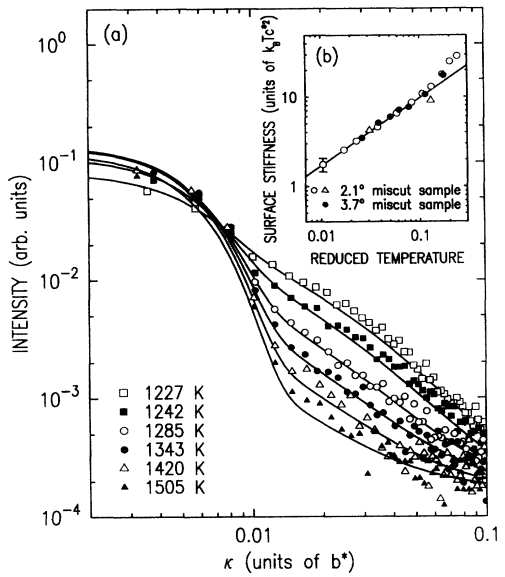

FIG. 4. (a) Log-log plot of the scattered intensity vs κ at $L = 2.0$ for several temperatures in the one-phase region. Solid lines correspond to the model described in the text. (b) Surface stiffness vs reduced temperature for the 2.1° miscut sample (open circles and open triangles) and the 3.7° miscut sample (solid circles). The solid line is a best fit to a power law for reduced temperatures less than 0.1.

dot-dashed line is a fit of these points using the same exponent as describes the phase boundary. We interpret this as a spinodal line, in analogy with the spinodal line that may be identified near the critical point of a liquid-gas system [12].

Several aspects of these results follow from the mean-field theory of Ref. [3]. Specifically, we take the free energy per unit area for surface misorientation θ to be

$$f(\theta) = f|\theta| + g_0(T - T_t)|\theta|^3 + h|\theta|^4. \quad (2)$$

Here, f is the free energy of an isolated step, while the $|\theta|^3$ and $|\theta|^4$ terms represent step interactions. Above T_t, the effective interaction between steps is repulsive; below T_t, the effective interaction is attractive at large step separations. Minimization of Eq. (2) with respect to θ leads to a tricritical point at T_t and a first-order phase boundary at $T^*(\theta) = T_t - 3h|\theta|/2g_0$. It is also possible to calculate the surface stiffness in the context of Eq. (2), following Ref. [11]. One predicts that the surface stiffness decreases according to $\tilde{\gamma} = \sqrt{6\Sigma g_0[T - T_s(\theta)]}$, where $T_s(\theta) = T^*(\theta) - h|\theta|/2g_0$ is the spinodal line, and Σ is the line tension of a single step. Clearly, the predicted behavior is qualitatively similar to that observed. However, the tricritical exponents for the shape of the coexistence curve and for the surface stiffness are given by mean-field theory as $\beta = 1$ and $\lambda = 1/2$, respectively. By contrast, we measure $\beta = 0.42 \pm 0.10$ and $\lambda = 0.76 \pm 0.20$.

As may be seen in Fig. 3, on cooling below T_3, the stepped phase peak, corresponding to an angle of 6.4° at T_3, is replaced by a peak corresponding to a misorientation angle of 5.7°. With further cooling, the position of this peak remains independent of temperature, consistent with its correspondence to the (114) facet. Therefore, for temperatures below T_3 the surface morphology is comprised of (114) facets in coexistence with (113) facets. The appearance of the (114) facet below T_3 stands outside Eq. (2). However, if the surface free energy of the (114) facet becomes lower with decreasing temperature relative to that of stepped (113) surfaces, then the observed behavior may be readily understood [5–7].

In summary, we have determined the orientational phase diagram of stepped Si(113) surfaces, tilted towards [001]. We have found a tricritical point at $T_t = 1223$ K, which separates a line of continuous orientational transformations from first-order faceting. We have characterized the tricritical scattering above T_t and the shape of the coexistence curve below T_t. Our results motivate renewed theoretical consideration of tricritical behavior in the orientational phase diagram, and of the microscopic origin of the direct attraction between steps, which is indicated.

We would like to thank D. Abernathy, L. Berman, D. Gibbs, B. McClain, G. Watson, and M. Yoon for enlightening discussions. Support provided by JSEP (DAAL-03-94-C-0001) and NSF (DMR 911965), and for X20A by NSF (DMR-9022933) and IBM, and for NSLS by the DOE (DE-AC0276CH00016).

[1] C. Rottman and M. Wortis, Phys. Rev. B **29**, 328 (1984).
[2] C. Jayaprakesh and W. F. Saam, Phys. Rev. B **30**, 3916 (1984).
[3] C. Jayaprakesh *et al.*, Phys. Rev. B **30**, 6549 (1984).
[4] C. Rottman *et al.*, Phys. Rev. Lett. **52**, 1009 (1984).
[5] R. J. Phaneuf and E. D. Williams, Phys. Rev. Lett. **58**, 2563 (1987); E. D. Williams and N. C. Bartelt, Science **251**, 273 (1991).
[6] J. C. Heyraud *et al.*, J. Cryst. Growth **98**, 355 (1989); P. Nozières, J. Phys. (Paris) **50**, 2541 (1989).
[7] G. M. Watson *et al.*, Phys. Rev. Lett. **71**, 3166 (1993); M. Yoon *et al.*, Phys. Rev. B **49**, 16 702 (1994).
[8] D. L. Abernathy, Ph.D. thesis, MIT, Cambridge, Massachusetts, 1993; D. L. Abernathy *et al.*, Phys. Rev. B **49**, 2691 (1994).
[9] B. S. Swarztentruber *et al.*, J. Vac. Sci. Technol. A **7**, 2901 (1989).
[10] M. K. Sanyal *et al.*, Phys. Rev. Lett. **66**, 628 (1991).
[11] See, for example, S. N. Coppersmith *et al.*, Phys. Rev. B **25**, 349 (1982).
[12] See, for example, G. B. Benedek, in *Polarization, Matter and Radiation* (Presses Universitaire de France, Paris, 1968), p. 49; B. Chu *et al.*, Phys. Rev. **185**, 219 (1969).